Spectrochimica Acta Part B: Atomic Spectroscopy 187 (2022) 106330

Contents lists available at ScienceDirect

Spectrochimica Acta Part B: Atomic Spectroscopy

journal homepage: www.elsevier.com/locate/sab

Exploiting dynamic reaction cell technology for removal of spectral interferences in the assessment of Ag, Cu, Ti, and Zn by inductively coupled plasma mass spectrometry

Cristian Suárez-Oubiña, Paloma Herbello-Hermelo, Pilar Bermejo-Barrera, Antonio Moreda-Piñeiro *

Trace Element, Spectroscopy and Speciation Group (GETEE), Institute of Materials iMATUS, Department of Analytical Chemistry, Nutrition and Bromatology, Faculty of Chemistry, Universidade de Santiago de Compostela, Avenida das Ciencias, s/n, 15782 Santiago de Compostela, Spain

ARTICLE INFO

Keywords:
Dynamic-reaction cell
Ammonium reaction gas
Inductively coupled plasma mass spectrometry
Interferences
On-mass approach
Mass shift approach

ABSTRACT

Analytical methods based on dynamic-reaction cell (DRC) technology using ammonia as a reaction gas have been developed for the determination of ultra-trace Ti, Zn, Cu and Ag by inductively coupled plasma mass spectrometry (ICP-MS). Challenging spectral interferences from complex matrices were demonstrated to be overcome by DRC, and several DRC approaches (on-mass and mass-shift) using ammonium (NH_3) as a reaction gas were assessed and compared to the standard or "vented" mode analysis. Ammonium cluster ions were generated for Ti, Cu, Zn, and Ag (mass shift approach). The on-mass approach was also explored to take advantage of collisional focusing phenomena. In addition, DRC operating conditions were optimised by modifying NH_3 gas flow rate and rejection parameter q (RPq). The optimised conditions were applied to show the usefulness of either on-mass or mass-shift approaches when removing Ca and P interferences. Finally, the sensitivity of all measurement modes was studied and excellent limits of detection (at few ng L^{-1} levels) were assessed.

1. Introduction

Inductively coupled plasma mass spectrometry (ICP-MS) has been demonstrated to be one of the leading techniques for elemental analysis, allowing for the determination of ultra-trace levels of metals and metalloids in a large variety of samples. ICP-MS offers many advantages over other spectrometric techniques, such as high sensitivity, wide linear dynamic range (nine orders of magnitude), and multi-element and isotopic-ratio measurement capabilities. Plasma source high temperature operation of about 7000 K allows all chemical bonds present in organic and inorganic compounds (even large biomolecules) to be readily broken, thus providing a more efficient atomization over other atomic based techniques.

Despite these advantages, ICP-MS also possesses some drawbacks. The occurrence of spectral (polyatomic and isobaric interferences) and non-spectral interferences are the most important shortcomings [1,2]. Polyatomic interferences are derived from plasma gas (typically Ar), sample matrix, atmospheric gas or solvent solution (water or organic solvents), and imply the generation of polyatomic species that coincidence at mass-charge ratio with the analyte. Several strategies have been developed to overcome ICP-MS interferences, including cold plasma conditions, mathematical correction equations, and improved mass analysers, such as sector field ICP-MS (SF-ICP-MS) [[3–7], and the use of collision-reaction cell (DRC) technology [8]. Although SF-ICP-MS has greatly improved the technical capabilities of ICP-MS and has allowed higher mass resolution than other mass analysers, it is not able to solve all interferences [4].

Cells in DRC are pressurized with a gas, and spectral interferences are removed by either selective reaction of the analyte and/or interfering ion with a reactive gas (typically H_2 [9], CH_4 [10], O_2 [11–13], CH_3F [14] and NH_3 [15,16]), or collisions of the ions with a non-reactive gas (typically He) in combination with kinetic energy discrimination (KED). The literature indicates that O_2 reaction gas has a high and predictable reactivity behaviour which implies high sensitivity [12,13]; whereas, CH_4 gas is inert to fight against possible matrix interferences (limited applications), and H_2 is especially useful for overcoming Ar interferences [9]. On the other hand, NH_3 and CH_3F reaction gases show a high and unpredictable reactivity and offer a wide range of possibilities

* Corresponding author.
E-mail address: antonio.moreda@usc.es (A. Moreda-Piñeiro).

https://doi.org/10.1016/j.sab.2021.106330
Received 19 October 2021; Received in revised form 17 November 2021; Accepted 19 November 2021
Available online 24 November 2021

Table 1
General (common) operating ICP-MS conditions.

Spray chamber type	Quartz cyclonic
PC^{3x} Peltier Cooler System	4 °C
Nebulizer Type	PFA MicroFlow
RF power (W)	1600
Plasma Gas Flow (L min^{-1})	15
Auxiliary Gas flow (L min^{-1})	1.2
Nebulizer Gas Flow (L min^{-1})	1.14
Sample uptake rate (μL min^{-1})	≈ 220
Acquisition Mode	Scanning
Dwell time per amu (ms)	50 ms
Quadrupole ion deflector (V)	Set for maximum ion transmission
Mass range (m/z)[a]	Ti: 35–200 Cu: 50–200 Zn: 50–200 Ag: 90–200
Sweeps	20
Readings	1
Replicates	3

[a] Specific conditions (ammonium flow rate, RPq, monitored m/z, ammonium adduct and mode analysis) are given in Table 2

(the formation of several adducts or ion-products) in contrast to only one adduct generated from O_2 gas. These features provide high selectivity for ICP-MS analysis with DRC technology using NH_3 and CH_3F as reaction gases.

NH_3 ionization energy is lower than that exhibited by most elements due to electrons free-pair, which make easier charge-transfer reactions [17,18], and shows lower reaction efficiency than other reaction gases. However, this lower reactivity is compensated by higher selectivity because several adducts containing more than one ammonium molecule can be formed, and thus mass-charge ratios of interest are shifted to a free-interference spectral region. In addition, the assessment of reaction gas flow rate and dynamic band pass ion guide, which involves Mathieu Parameters (RPq and RPa values), are also required. Formation of new species (potentially new interferences) in the cell could be controlled when a reactive gas is used, and dynamic band pass optimization must be assessed through rejection parameters [8].

In this work we aim to develop several NH_3-based DRC methods for ultra-trace determination of Ti, Zn, Cu and Ag. These elements, except Ag, have been reported to be subjected to interference by large concentrations of Na, P, S, Ca and Mg (elements typically found in biological samples, seafood included [13,19–21]),. The comprehensive evaluation takes into account the NH_3 flow rate and DRC parameters influence on analytes to find the best conditions both for on-mass (monitoring of the original elemental mass) and mass-shift (monitoring NH_3-based adducts) approaches. Furthermore, the most common interferences in seafood matrices, such as Ca and P, were also evaluated.

2. Experimental

2.1. Instrumentation

Analysis were performed using a NexION 2000 DRC-ICP-MS (Perkin Elmer, Waltham, MA, USA) equipped with a Single Cell Micro DX autosampler (Perkin Elmer), and the Syngistix™ ICP-MS 2.5 version software (Perkin Elmer). In addition, the instrument was operated with a PFA MicroFlow nebulizer and a cyclonic spray chamber (Glass Expansion, Inc., Melbourne, Australia), a quartz torch with a quartz injector tube (2.5 mm i.d.), and triple cone equipment with nickel sampler cone, skimmer cone and hyperskimmer cone.

2.2. Reagents and standards

Ultrapure water (18.2 MΩ cm of resistivity) was obtained from a Milli-Q® IQ 7003 purification device system from Millipore (Bedford, MA, USA). Mono-elemental 1000 mg L^{-1} standards of titanium $[(NH_4)_2TiF_6]$, copper $[Cu(NO_3)_2]$, and silver($AgNO_3$) were purchased from Perkin Elmer. Mono-elemental standards of zinc $[Zn(NO_3)_2]$ and calcium $[Ca(NO_3)_2]$ were from Merck (Darmstadt, Germany), and phosphorus ($NH_4H_2PO_4$) was from Scharlau (Barcelona, Spain). NexIONSetup Solution, 10 μg L^{-1}Be, In, U, and Ce, was from Perkin Elmer. Hyperpure nitric acid 69% (*w/v*) was from Panreac (Barcelona, Spain). Argon (99.998%) and ammonium (99,999%) were from Nippon Gases (Madrid, Spain).

Glassware and plastic ware was decontaminated by soaking in 10% (*v*/v) nitric acid for at least 48 h. Material was then rinsed with ultra–pure water several times.

2.3. ICP-MS measurements

ICP-MS settings and parameters are detailed in Table 1. Daily performance was assessed by monitoring Be, In, U, and Ce (1.0 μg L^{-1} each one) and verifying intensities higher than 4500 counts s^{-1} (Be), 80,000 counts s^{-1} (In), and 60,000 counts s^{-1} (U), and a background (mass-to-charge ratio of 202) lower than 3.0, and Ce++/Ce and CeO/Ce ratios lower than 3.0 and 2.5%, respectively.

Calibration, covering Ti, Ag, Zn, and Cu concentrations within the 0.1–10 μg L^{-1}range (five level concentrations) was prepared in 1.0% (*v*/v) nitric acid. Reagent blanks (1.0% (v/v) nitric acid) were also analysed throughout the work.

2.4. Data treatment

Spectra Analysis was performed using Origin8 Pro Software (Northampton, MA, USA). Data and graph peaks analysis was also performed using Origin8 Pro from Excel exported Data from Syngistix™ ICP-MS 2.5 software (Perkin Elmer).

3. Results and discussion

As previously mentioned, ammonium shows no predictable reactivity for forming suitable ion products, shifting these ammonium clusters to a free-interference spectral region at higher mass-charge ratios. This fact makes ammonium gas the best option to face interferences in challenging matrices [15]. Several researches have reported two available approaches for DRC technology: on-mass mode working at mass-charge elemental ratio, and shift-mass mode working at mass-charge ratio displaced to another region of the mass spectra (monitoring the formed ion products) [15,22]. In some cases, mass-shift mode could be a more appealing methodology than the on-mass approach in order to avoid interferences. However, sensitivity and measurement stability are also important factors to be taken into account, and they can lead us to consider on-mass approaches as the most suitable strategy in some specific cases.

Ammonium gas generally reacts with elements through charge-transfer reactions to form several adducts by addition of groups such as (—H), (-NH), ($-NH_2$), and mainly ($-NH_3$). The number of groups can be more than one depending on the ammonium flow added and the element's chemical properties. Moreover, especial attention to other possible reactions inside the reaction cell, such as ion products derived from Ar supply and/or from the matrix sample, must be considered. This issue can be solved considering the isotopic pattern or the isotopic ratio of elements because if both isotopes behave equally, we can conclude without doubt that measurements include only the analyte (element) of interest.

3.1. Selection of the best ion-products

The first step to develop a DRC based ICP-MS method is the selection of the ion products (adducts), and the optimization of the formation conditions by selecting the appropriate ammonium flow rate, among others [17,22]. The most suitable ion product for each element has been

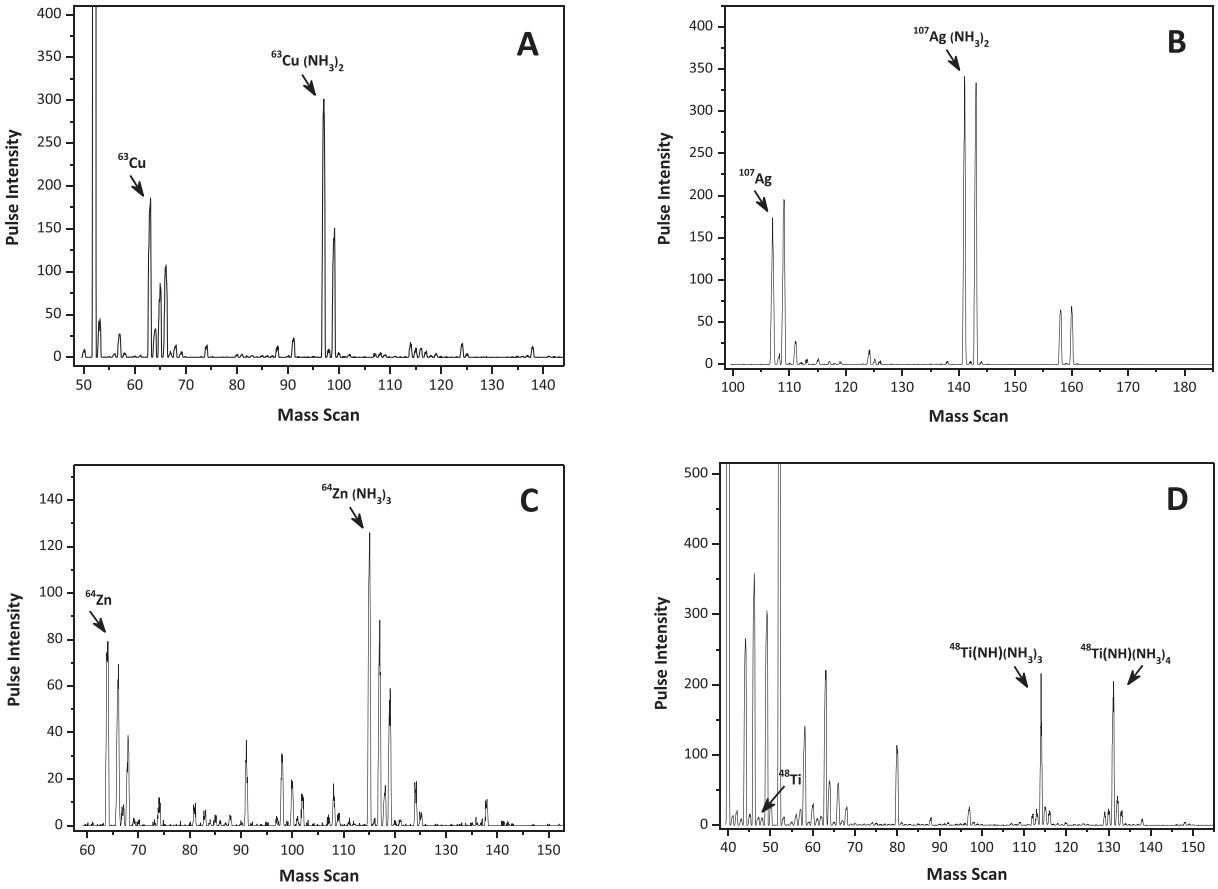

Fig. 1. Mass spectra illustrating compounds that are formed with ammonium: (A) Cu, 1.5 mL min^{-1}, (B) Ag, 2.5 mL min^{-1}, (C) Zn, 2.0 mL min^{-1}, and (D) Ti, 1.0 mL min^{-1}.

performed by scanning over a wide mass range between the elemental mass-charge ratio and a mass-charge ratio that allows the inclusion of numerous ammonium molecules [11]. Cu, Zn, Ag, and Ti standards (5 μg L^{-1} in 1.0%(*v*/v) nitric acid) were used to perform single element mass scanning (ICP-MS operating conditions in Table 1) at ammonium flow rates of 0.5, 1.0, 1.5, 2.0, 2.5, and 3.5 mL min^{-1}. Figure 1 shows the mass spectra for each element at the best ammonium flow rate: 1.5 mL min^{-1}for Cu (A), 2.0 mL min^{-1} for Zn (B), 2.5 mL min^{-1} for Ag (C), and 1.0 mL min^{-1} for Ti (D). The highest incidence of spectral interferences for Cu, Zn and Ti were observed at the smaller mass-charge ratio regions; whereas, the several adducts produced at large mass-charge ratios were free of spectral interferences (Fig. (A, B,D)). Fig. S1 (electronic supplementary information, ESI) shows the complete set of mass spectra for Cu, Zn, Ti, and Ag at the different ammonium flow rates tested. A general trend that can be extracted from these mass spectra is the ability to focus the original mass-charge ratios when using ammonium flow rates lower than 0.5 mL min^{-1}, conditions which lead to obtaining original mass-charge ratios of higher intensity. This effect is referred to as collisional focusing [11,23] and will be studied in greater detail in the following sections. Another general conclusion that can be drawn is the dilution effect at relatively high gas flows, which becomes evident from flow rates of 2.0 mL min^{-1} (spectral interferences are more efficiently eliminated, but sensitivity is impaired). Finally, isotopic pattern from ^{49}Ti-based ammonium adducts were not observed (Figure 1D) since the very low abundance of this isotope (5.41%) versus ^{48}Ti (73.72%).

Therefore, the best ion products (mass-shift approach) were ^{63}Cu(NH$_3$)$_2$ (mass-charge ratio of 97), ^{65}Cu(NH$_3$)$_2$ (mass-charge ratio of 99), ^{64}Zn(NH$_3$)$_3$ (mass-charge ratio of 115), ^{66}Zn(NH$_3$)$_3$ (mass-charge ratio of 117), ^{107}Ag(NH$_3$)$_2$ (mass-charge ratio of 141), ^{109}Ag(NH$_3$)$_2$ (mass-charge ratio of 143), ^{48}Ti(NH)(NH$_3$)$_3$ (mass-charge ratio of 114), and ^{48}Ti(NH)(NH$_3$)$_4$ (mass-charge ratio of 131). Regarding Ti, the selected ammonium adducts are different from those proposed by other authors, for example, ^{48}Ti(NH$_3$)$_6$(*m*/*z* 150) [17–19] and ^{48}TiNH$_2$(NH$_3$)$_4^+$(m/z 132) [24] for ICP-MS measurements, and ^{48}Ti(NH) (m/z 63) for single particle (SP-ICP-MS [25]. The ammonium flow rate and, probably, the design of the collision/reaction cell, have influence on the formation of ammonium adducts.

3.2. Optimization of ammonia flow rate

The effect of the ammonium flow rate was evaluated at the selected adducts (mass-shift approach) and original mass-charge ratios (on mass approach). The RPq Mathieu parameter was fixed at 0.25 throughout the experiment. Results after scanning each mass-charge ratio are plotted in Figure 2. The isotopic ratio at each elemental mass was used for verifying that the element (element mass) of interest was being measured and for ensuring the minimum influence of the matrix components on the ion products formed from the most abundant isotopes.

Mass-charge ratios from Cu, Ag, and Zn show a similar behaviour (Figure 2). The highest intensities were obtained at the lowest flow rate tested (0.5 mL min^{-1}) for the elemental masses. As previously mentioned, this effect is attributed to the collisional focusing phenomena, which allows sensitive on-mass assessments [11]. The formation of adducts at higher ammonium flow rates were optimum at 1.5 mL min^{-1} for Cu, which led to the formation of ^{63}Cu(NH$_3$)$_2$ and ^{65}Cu(NH$_3$)$_2$ adducts (mass-charge ratios of 97 and 99, respectively). Other ion products for Cu were not found even at the high ammonium flow rate, which is in good agreement with the published literature [24]. In the case of Ag, the most prevalent ion products were ^{107}Ag(NH$_3$)$_2$ and ^{109}Ag(NH$_3$)$_2$ (mass-charge ratios of 141 and 143, respectively), with maximum intensities at

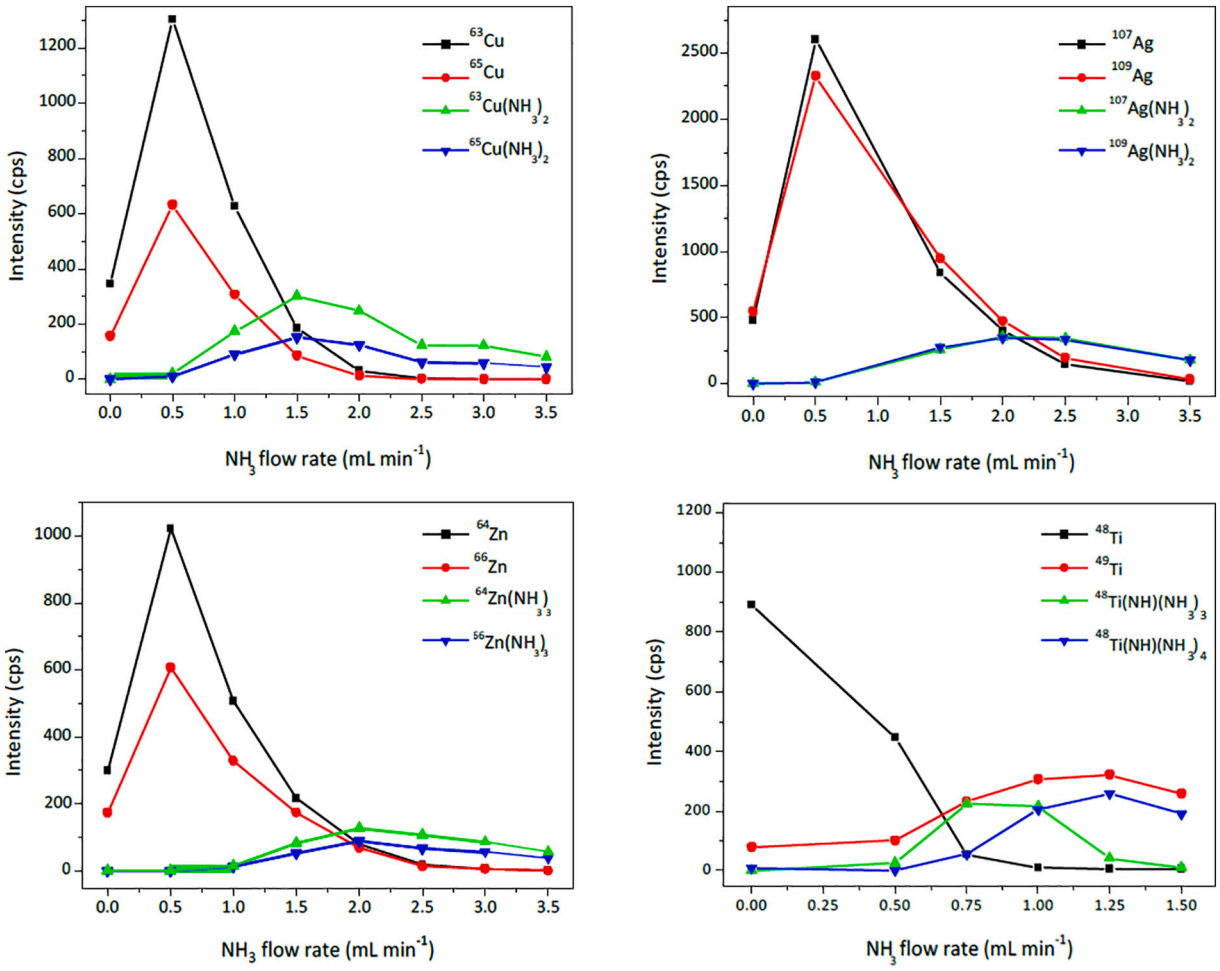

Fig. 2. Effect of the ammonium flow rate on target's intensities (mass-shift approach).

Table 2
Optimum conditions for standard, mass-shift, and on-mass modes for Ti, Cu, Zn, and Ag determination.

Analyte	Monitored adduct	Monitored *m/z*	Mode analysis	NH_3 Flow rate (mL min^{-1})	RPq value
Ti	$Ti(NH)(NH_3)_3$	114	Mass-shift	1.0	0.2
	$Ti(NH)(NH_3)_4$	131	Mass-shift	1.0	0.2
	Ti	48	Standard	–	0.25
	Cu	63	On-mass	0.5	0.35
Cu	$Cu(NH_3)_2$	97	Mass-shift	1.5	0.2
	Cu	63	Standard	–	0.25
	Zn	64	On-mass	0.5	0.35
Zn	$Zn(NH_3)_3$	115	Mass-shift	2.0	0.2
	Zn	64	Standard	–	0.25
	Ag	107	On-mass	0.5	0.35
Ag	$Ag(NH_3)_2$	141	Mass-shift	2.0	0.2
	Ag	107	Standard	–	0.25

flow rates within the 2.0–2.5 mL min^{-1} range (a flow rate of 2.0 mL min^{-1} was selected due to lower ammonium gas consumption). Finally, ion products from Zn ($^{64}Zn(NH_3)_3$ and $^{66}Zn(NH_3)_3$, mass-charge ratios of 115 and 117, respectively) showed lower intensities than those observed for Cu and Ag ion products, which implies that the mass shift approach for Zn determination is less sensitive than the on-mass approach. The highest intensities of $^{64/66}Zn(NH_3)_2$ adducts were observed at an ammonium flow rate of 2.0 mL min^{-1}.

Regarding Ti, the elemental masses (^{48}Ti and ^{49}Ti) intensities are low when using lower ammonium flow rates, mainly for ^{49}Ti. Ammonium clusters from ^{49}Ti were not observed because the very low abundance of this isotope; however, adducts from ^{48}Ti, such as $^{48}Ti(NH)(NH_3)_3$ and $^{48}Ti(NH)(NH_3)_4$ (mass-charge ratio of 114 and 131, respectively), were observed at ammonium flow rates between 0.75 and 1.25 mL min^{-1} (1.0 mL min^{-1}finally selected). Additionally, a Ti(NH) ion product was found to be formed in the cell but was discarded because the short mass-charge ratio is not useful [25].

Table 2 summarises the selected ammonium flow rate and ion products for mass-shift approaches, as well the selected flow rate for the on-mass assays (a further re-optimization will be performed by verifying the on-mass results).

3.3. Optimization of rejection parameter q value

Mathieu parameters, also called rejection parameters (RPq and RPa) are defined as a stabilized mass band-pass which controls both low-mass cut-off and high-mass cut-off limits, respectively [13]. The influence of these parameters on the reaction cell must be controlled in order to remove the transmitted ions which are outside these stabilization limits [9,13].

The influence of the RPq on mass-shift and on-mass approaches was evaluated after fixing the RPa at 0, the axial field voltage (AFT) at 350 V (default values), and the deflector voltage at the specific element mass in the quadrupole ion deflector to achieve maximum ion transmission in the reaction cell. In addition, the ammonium flow rate was fixed at the previous optimised values: 0.5 and 2.0 mL min^{-1} for Ag and Zn when

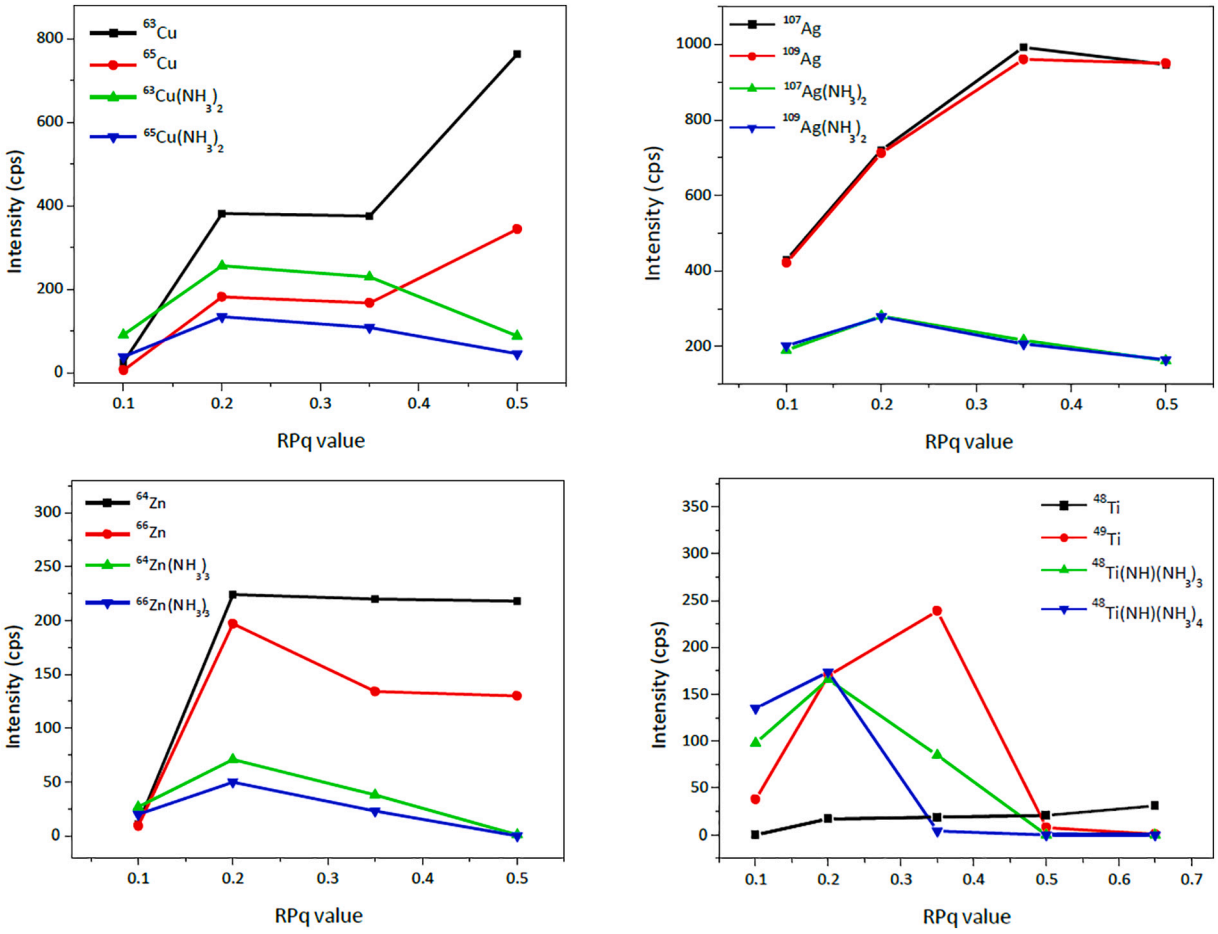

Fig. 3. Effect of the RPq on the target's intensities (measurements were done for each element at its optimised ammonium flow rate values).

using the on mass and mass shift approaches, respectively; 0.5 and 1.5 mL min^{-1} for Cu when using the on mass and mass shift approaches, respectively; and 1.0 mL min^{-1} for Ti (mass shift approach). Figure 3 shows that higher intensities are obtained at high RPq values when using the on-mass approach (elemental masses). This is because high RPq values respect shorter masses (elemental ions), allowing for an efficient confinement of the elemental ions in the cell, and hence higher sensitivity. In addition, Figure 3 shows very low signals for ^{48}Ti (values lower than those measured for the less abundant isotope ^{49}Ti). The explanation is because most of ^{48}Ti is efficiently transformed into the $^{48}Ti(NH)(NH_3)_3$ and $^{48}Ti(NH)(NH_3)_4$ ammonium adducts at an ammonium flow rate of 1.0 mL min^{-1}.

Regarding the mass shift approach, the confinement of ion products is favoured at low RPq values because high RPq values with respect to large masses (ammonium clusters) leads to exclusion of the shorter masses (the elemental masses) minimizing the further formation of the ammonium adducts. Therefore, an RPq value of 0.2 was selected for all analytes when using the mass shift approach (Table 2). Regarding on-mass approaches, the selection of the RPq will be done after optimising the collisional focussing phenomena.

3.4. Collisional focusing phenomena

As previously mentioned, improvements (increases) on the elemental ion intensities are obtained when using small ammonium flow rates (on-mass approach) with respect to the standard working mode (vented mode). This fact is attributed to the collisional focusing effect in instruments with collision/reaction cells as a consequence of ion confinement (longer traveling path in the ion guide) due to energy losses by several collisions in the cell [11,23]. The phenomena has been reported for gases such as O_2 [17,23], H_2 [11], CH_4 [10] and NH_3 [15,16], and the magnitude is dependent on the monitored ion and the gas (higher loss of ion kinetic energy per collision for heavier gases) [11,23].

Therefore, cell conditions (ammonium flow rate and RPq) were re-evaluated (closer ammonium flow rate and RPq conditions) at the selected elemental ions for on-mass determinations. First, ammonium flow rates of 0.1, 0.3, 0.5 y 0.7 mL min^{-1} were tested at a constant RPq of 0.25 (RPa at 0 and AFT at 350 V). Fig. S2 (ESI) shows a clear increase on the signal for Cu, Zn and Ag isotopes at low ammonium flow rates, with a maximum value at 0.5 mL min^{-1}. Moreover, intensities when using ammonium were found to be quite higher than those obtained by using the standard mode (absence of ammonium gas). However, the trend is different for Ti (Fig. S2, ESI), and the on-mass approach is not advantageous (higher sensitivity was obtained when using the standard mode).

The effect of the RPq Mathieu parameter was studied for Cu, Zn and Ag (most abundant isotopes for verifying that the isotopic pattern is met) at an ammonium flow rate of 0.5 mL min^{-1}. In addition, the potential ion products formed were also registered. Maximum intensities were observed with RPq of 0.5 for Cu elemental masses, and 0.35 for Zn and Ag; whereas, intensities of the ammonium cluster adducts were negligible (Fig. S3, ESI). However, Cu intensities at 0.35 and 0.5 RPq are similar (Fig. S3, ESI), and an RPq of 0.35 can also be selected for Cu ion monitoring.

Results regarding flow rate and RPq (on-mass mode) have been similar to those previously obtained (section 3.3 and 3.4), and on-mass conditions for Cu, Zn and Ag were established at 0.5 mL min^{-1} for ammonium flow rate and 0.35 for RPq (Table 2).

Table 3
Isotopes of interest and major polyatomic spectral interferences derived from fish matrix.

Isotope	Major spectral interferences
^{48}Ti	$^{31}P^{17}O$, ^{48}Ca, $^{32}S^{16}O$
^{63}Cu	$^{31}P^{16}O_2$, $^{46}Ca^{16}O^1H$, $^{23}Na^{40}Ca$
^{64}Zn	$^{48}Ca^{16}O$, $^{36}Ar^{14}N_2$, $^{32}S^{16}O_2$, $^{31}P^{16}O^{17}O$, $^{31}P^{16}O_2$ ^1H
^{107}Ag	Minimum interference

3.5. Interferences study: removal of calcium and phosphorus interferences

DRC technology could be an appealing solution [9,14,22,26] when assessing elements exhibiting low mass-charge ratios in biological matrices by ICP-MS because potential spectral interferences derived from major elements (Mg, K, Na, Ca and P) [12,13,19,20] are efficiently removed/minimised. As shown in Table 3, Ca and P are potential interferences when assessing Ti and Zn by ICP-MS, and the optimised DRC conditions (on-mass and mass shift approaches) have therefore been tested to know the possibility of a free-interference determination. The on-mass approach (^{63}Cu and ^{64}Zn) and standard mode (^{63}Cu, ^{64}Zn, and ^{48}Ti) measurements were performed with the most abundant isotopes; whereas, the mass shift approach was carried out with $^{63}Cu(NH_3)_2$ (mass-charge ratio of 97), $^{64}Zn(NH_3)_3$ (mass-charge ratio of 115), $^{48}Ti(NH)(NH_3)_3$ (mass-charge ratio of 114), and $^{48}Ti(NH)(NH_3)_4$ (mass-charge ratio of 131). Experiments regarding silver were not performed since this element does not show significant spectral interferences (Table 3).

Taking into account the levels of Ca and P in seafood, the study was performed with increasing Ca and P concentrations up to 50 mg L^{-1}. Figure 4 shows that Ca at concentrations higher than 5 mg L^{-1} causes a serious interference when using the standard mode (analytical recoveries close to 500% at the highest Ca concentration level). The mass

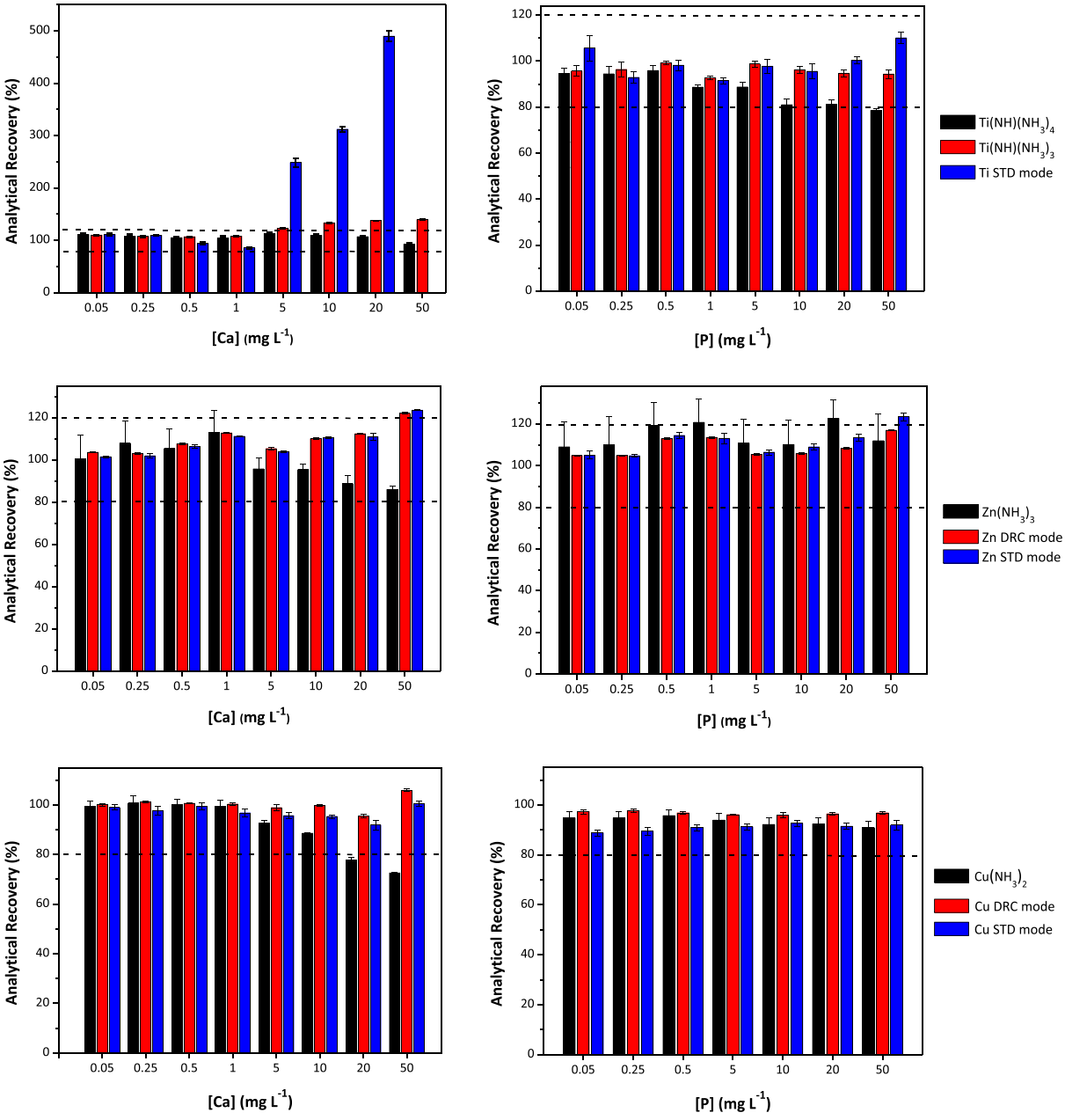

Fig. 4. Effect of Ca and P concentration on analytical recoveries for Ti, Cu and Zn when using the standard mode, on-mass approach and mass-shift approach. Mass-shift mode with two Ti adducts were used.

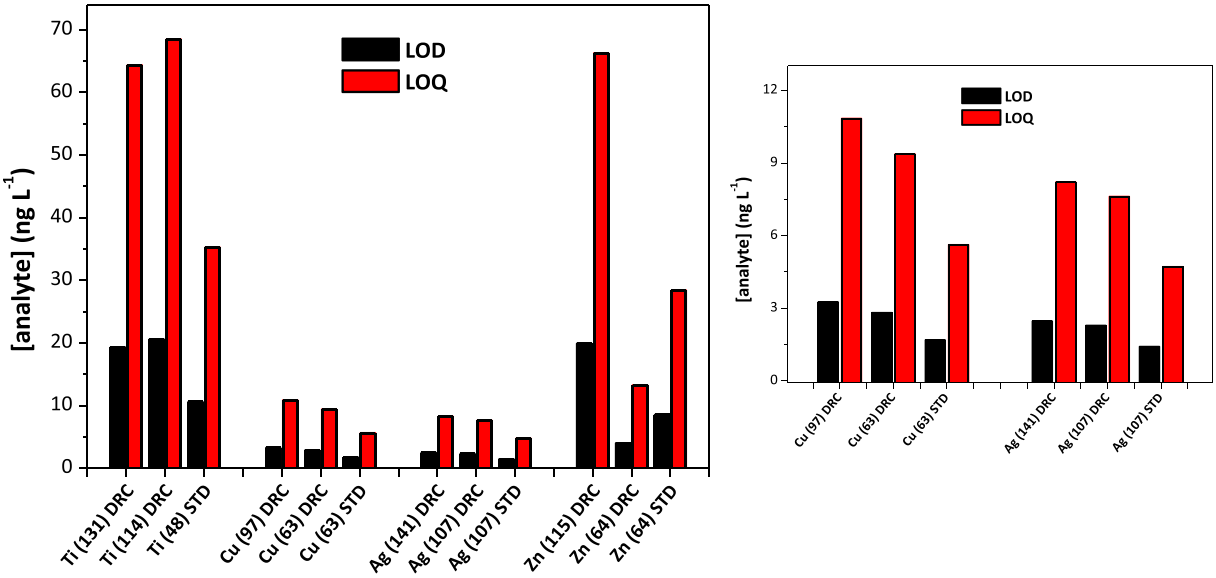

Fig. 5. LOD and LOQ values obtained for Ag, Ti, Cu and Zn with the standard mode, on-mass and mass shift approaches.

shift approach using both $^{48}Ti(NH)(NH_3)_3$ and $^{48}Ti(NH)(NH_3)_4$ adducts was found to be successful for Ca interference removal (Ti analytical recoveries within the 80–120% range). The P interference on Ti was less important, and standard and mass shift measurements were found adequate. However, analytical recoveries slightly lower than 80% were obtained when using the $^{48}Ti(NH)(NH_3)_4$ adduct (mass shift approach, Figure 4).

Similarly to Ti, the interference of Ca on Zn was more notorious than P, and the interference from the latter was successfully compensated when working with the standard mode and also with the on-mass and mass shift ($^{64}Zn(NH_3)_3$ adduct) approach. Regarding Ca interference, the three measurement modes work properly (quantitative analytical recoveries), but both the standard and on-mass mode were found to give Zn analytical recoveries slightly above 120% at the highest Ca level tested.

Finally, Cu experiments (Figure 4) showed the convenience of the on-mass approach for overcoming the Ca interference; whereas, the mass shift approach ($Cu(NH_3)_3$ adduct) falls at Ca concentrations higher than 10 mg L^{-1}.

3.6. Sensitivity study

The limit of detection (LOD) and the limit of quantification (LOQ) have been calculated based on the 3 SD/m and 10 SD/m criterion (*SD*, the standard deviation of eleven measurements of the blank; and *m*, the slope of a calibration graph within the 1.0–10 μg L^{-1} range). Calibration graphs were found to exhibit $r^2 > 0.999$, and the RSD% of the blank measurements were always below 4%, except for mass shift ($Zn(NH_3)_3$ adduct) for Zn (RSD within the 9–12% range). The impaired precision for Zn is related to inefficiencies on the ammonium adduct formation (lower intensities and wider peaks than those found for other metal adducts). Figure 5 shows the assessed LOD/LOQ values by using the standard mode and the on-mass and mass shift approaches. In general, higher LOD/LOQ values are obtained for DRC technology (on-mass and mass shift) than for the standard measurement mode since the use of the reaction gas implies a certain dilution. Similar LOD/LOQ were attained for Ti when using the mass shift by monitoring both $^{48}Ti(NH)(NH_3)_3$ and $^{48}Ti(NH)(NH_3)_4$ adducts. The sensitivity (LOD close to 20 ng L^{-1} and LOQ close to 65 ng L^{-1}) were higher than those reported by Fu et al. (lower than 1 and 3 ng L^{-1}, respectively, when using NH_3/He and a NH_3/H_2/He mixtures and tandem mass technology) [18]. Similar LOD values (20 ng L^{-1}) for Ti in blood serum have been reported for DRC technology using the $^{48}Ti(NH_3)_6$ adduct (mass-charge ratio of 150) [19].

In the case of Cu and Ag, similar sensitivity was achieved when working with the on-mass and mass shift approaches; whereas, the on-mass mode was found to be more sensitive for Zn than the mass shift approach ($Zn(NH_3)_3$ adduct) and even than the standard mode (Figure 5). Improved sensitivity of the on-mass mode against the mass shift approach can be related to the lack of efficiency in the formation of the $Zn(NH_3)_3$ adduct. Higher sensitivity for on-mass Zn assessment than the standard mode could be attributed to the efficient collisional focusing phenomena. The obtained LOD/LOQ values for Cu, Zn and Ag (standard mode) are lower (LOD/LOQ of 1.7/5.6, 8.5/28.4, and 1.4/4.7 ng L^{-1} for Cu, Zn, and Ag, respectively) than those previously reported for these elements using ICP-MS with collision/reaction cell technology under standard mode (LOD/LOQ of 165/515, 19/63, and 9/32 ng L^{-1} for Cu, Zn, and Ag, respectively) [16]. Moreover, both on-mass and mass shift approches for Cu and Zn have also led to lower LOD/LOQ than the reported values [16]. Finally, sensitivity for Cu (on-mass and mass shift approaches, LOD/LOQ of 1.7/3.2 and 5.6/10.8 ng L^{-1}, respectively) is quite better than previous reported studies based on on-mass measurement mode with ammonium as a reaction gas (280 ng L^{-1}) [[27]].

4. Conclusions

DRC technology has been demonstrated to be a useful tool for facing challenging polyatomic and isobaric interferences in ICP-MS determinations. The use of ammonium as a reaction gas has allowed the development of methods based on mass shift and on-mass approaches. The sensitivity and selectivity have been found to be dependent on the measurement mode as well as the element itself. Ti free-interference determination (high selectivity) can be performed using the mass shift approach with moderate sensitivity; whereas, the on-mass approach has been found more suitable for Zn determination due to lack of efficiency on the formation of ammonium-Zn adducts. However, on-mass and mass shift approaches were found to give similar performances (selectivity and sensitivity) for Cu determination. Finally, a careful optimization of Mathieu parameters is needed for both on-mass and mass shift approaches, but it becomes quite important for on-mass methods due to the great (positive) influence of the collisional focusing phenomena on sensitivity.

Declaration of Competing Interest

The authors declare that they have no known competing financial interests or personal relationships that could have appeared to influence the work reported in this paper.

Acknowledgements

The authors wish to acknowledge the financial support of the *Ministerio de Economía y Competitividad, Gobierno de España* (project INNOVANANO, reference RT2018-099222-B-100), and the Xunta de Galicia (*Grupo de Referencia Competitiva*, grant number ED431C2018/19).

Appendix A. Supplementary data

Supplementary data to this article can be found online at https://doi.org/10.1016/j.sab.2021.106330.

References

[1] R.F.J. Dams, J. Goossens, L. Moens, Spectral and non-spectral interferences in inductively coupled plasma mass-spectrometry, Mikrochim. Acta. 119 (1995) 277–286, https://doi.org/10.1007/BF01244007.
[2] S.H. Tan, G. Horlick, Background spectral features in inductively coupled plasma/mass spectrometry, Appl. Spectrosc. 40 (1986) 445–460, https://doi.org/10.1366/0003702864508944.
[3] N. Jakubowski, L. Moens, F. Vanhaecke, Sector field mass spectrometers in ICP-MS, Spectrochim. Acta Part B, At. Spectrosc. 53 (1998) 1739–1763, https://doi.org/10.1016/S0584-8547(98)00222-5.
[4] N. Jakubowski, T. Prohaska, L. Rottmann, F. Vanhaecke, Inductively coupled plasma- and glow discharge plasma-sector field mass spectrometry: part I. tutorial: fundamentals and instrumentation, J. Anal. At. Spectrom. 26 (2011) 693–726, https://doi.org/10.1039/c0ja00161a.
[5] I. Rodushkin, E. Engström, A. Stenberg, D.C. Baxter, Determination of low-abundance elements at ultra-trace levels in urine and serum by inductively coupled plasma-sector field mass spectrometry, Anal. Bioanal. Chem. 380 (2004) 247–257, https://doi.org/10.1007/s00216-004-2742-7.
[6] J.M. Harrington, D.J. Young, A.S. Essader, S.J. Sumner, K.E. Levine, Analysis of human serum and whole blood for mineral content by ICP-MS and ICP-OES: development of a mineralomics method, Biol. Trace Elem. Res. 160 (2014) 132–142, https://doi.org/10.1007/s12011-014-0033-5.
[7] K. Sakata, K. Kawabata, Reduction of fundamental polyatomic ions in inductively coupled plasma mass spectrometry, Spectrochim. Acta part B, At. Spectrosc. 49 (1994) 1027–1038, https://doi.org/10.1016/0584-8547(94)80088-X.
[8] S.D. Tanner, V.I. Baranov, D.R. Bandura, Reaction cells and collision cells for ICP-MS: a tutorial review, Spectrochim. Acta part B, At. Spectrosc. 57 (2002) 1361–1452, https://doi.org/10.1016/S0584-8547(02)00069-1.
[9] A.S. Henn, F.S. Rondan, M.F. Mesko, P.A. Mello, M. Perez, J. Armstrong, L. A. Bullock, J. Parnell, J. Feldmann, E.M.M. Flores, Determination of Se at low concentration in coal by collision/reaction cell technology inductively coupled plasma mass spectrometry, Spectrochim. Acta Part B, At. Spectrosc. 143 (2018) 48–54, https://doi.org/10.1016/j.sab.2018.02.014).
[10] E. Soriano, V. Yusà, A. Pastor, M. de la Guardia, Dynamic reaction cell inductively couple plasma-mass spectrometry optimization for seawater analysis, Microchem. J. 137 (2018) 363–370, https://doi.org/10.1016/j.microc.2017.11.015.
[11] E. Bolea-Fernandez, D. Leite, A. Rua-Ibarz, L. Balcaen, M. Aramendía, M. Resano, F. Vanhaecke, Characterization of SiO2 nanoparticles by single particle-inductively coupled plasma-tandem mass spectrometry (SP-ICP-MS/MS), J. Anal. At. Spectrom. 32 (2017) 2140–2152, https://doi.org/10.1039/c7ja00138j.
[12] S. Li, Z. Yang, J. Cao, B. Qiu, H. Li, Determination of metallothionein isoforms in fish by cadmium saturation combined with anion exchange HPLC-ICP-MS, Chromatographia 81 (2018) 881–889, https://doi.org/10.1007/s10337-018-3523-3.
[13] Z.S. Gong, R. Yang, C.Q. Sun, W.N. Han, X.H. Jiang, S.X. Xu, Y. Wang, Simultaneous determination of P and S in human serum, blood plasma and whole blood by ICP-MS with collision/reaction cell technology, Int. J. Mass Spectrom. 445 (2019), 116193, https://doi.org/10.1016/j.ijms.2019.116193.
[14] S. Candás-Zapico, D.J. Kutscher, M. Montes-Bayón, J. Bettmer, Single particle analysis of TiO_2 in candy products using triple quadrupole ICP-MS, Talanta. 180 (2018) 309–315, https://doi.org/10.1016/j.talanta.2017.12.041.
[15] E. Bolea-Fernandez, D. Leite, A. Rua-Ibarz, T. Liu, G. Woods, M. Aramendia, M. Resano, F. Vanhaecke, On the effect of using collision/reaction cell (CRC) technology in single-particle ICP-mass spectrometry (SP-ICP-MS), Anal. Chim. Acta 1077 (2019) 95–106, https://doi.org/10.1016/j.aca.2019.05.077.
[16] Z.S. Gong, X.H. Jiang, C.Q. Sun, Y.P. Tian, G.H. Guo, Y.Z. Zhang, X.H. Zhao, Y. Wang, Determination of 21 elements in human serum using ICP-MS with collision/reaction cell, Int. J. Mass Spectrom. 423 (2017) 20–26, https://doi.org/10.1016/j.ijms.2017.10.001.
[17] L. Balcaen, E. Bolea-Fernandez, M. Resano, F. Vanhaecke, Inductively coupled plasma - tandem mass spectrometry (ICP-MS/MS): a powerful and universal tool for the interference-free determination of (ultra)trace elements - A tutorial review, Anal. Chim. Acta 894 (2015) 7–19, https://doi.org/10.1016/j.aca.2015.08.053.
[18] L. Fu, S.-Y. Shi, J.-C. Ma, Accurate determination of harmful and doping elements in soft magnetic ferrite powders using inductively coupled plasma tandem mass spectrometry, Chinese, J. Anal. Chem. 47 (2019) 1382–1389, https://doi.org/10.1016/S1872-2040(19)61189-8.
[19] L. Balcaen, E. Bolea-Fernandez, M. Resano, Accurate determination of ultra-trace levels of Ti in blood serum using ICP-MS/MS, Anal. Chim. Acta 809 (2014) 1–8, https://doi.org/10.1016/j.aca.2013.10.017.
[20] B. Markiewicz, A. Sajnóg, W. Lorenc, A. Hanć, I. Komorowicz, J. Suliburska, R. Kocyłowski, D. Barałkiewicz, Multielemental analysis of 18 essential and toxic elements in amniotic fluid samples by ICP-MS: full procedure validation and estimation of measurement uncertainty, Talanta. 174 (2017) 122–130, https://doi.org/10.1016/j.talanta.2017.05.078.
[21] I.F. Seregina, K. Osipov, M.A. Bolshov, D.G. Filatova, S.Y. Lanskaya, Matrix interference in the determination of elements in biological samples by inductively coupled plasma–mass spectrometry and methods for its elimination, J. Anal. Chem. 74 (2019) 182–191, https://doi.org/10.1134/S1061934819020114.
[22] T. Van Acker, E. Bolea-Fernandez, E. De Vlieghere, J. Gao, O. De Wever, F. Vanhaecke, Laser ablation-tandem ICP-mass spectrometry (LA-ICP-MS/MS) imaging of iron oxide nanoparticles in Ca-rich gelatin microspheres, J. Anal. At. Spectrom. 34 (2019) 1846–1855, https://doi.org/10.1039/c9ja00135b.
[23] N. Yamada, Kinetic energy discrimination in collision/reaction cell ICP-MS: theoretical review of principles and limitations, Spectrochim. Acta Part B, At. Spectrosc. 110 (2015) 31–44, https://doi.org/10.1016/j.sab.2015.05.008.
[24] L. Fu, S. Shi, X. Chen, H. Xie, Analysis of impurity elements in high purity cobalt powder by inductively coupled plasma tandem mass spectrometry, Microchem. J. 139 (2018) 236–241, https://doi.org/10.1016/j.microc.2018.03.002.
[25] M. Tharaud, A.P. Gondikas, M.F. Benedetti, F. Von Der Kammer, T. Hofmann, G. Cornelis, TiO_2 nanomaterial detection in calcium rich matrices by spICPMS. A matter of resolution and treatment, J. Anal. At. Spectrom. 32 (2017) 1400–1411, https://doi.org/10.1039/c7ja00060j.
[26] P. Petrov, B. Russell, D.N. Douglas, H. Goenaga-Infante, Interference-free determination of sub ng kg^{-1} levels of long-lived ^{93}Zr in the presence of high concentrations (μg kg^{-1}) of ^{93}Mo and ^{93}Nb using ICP-MS/MS, Anal. Bioanal. Chem. 410 (2018) 1029–1037, https://doi.org/10.1007/s00216-017-0635-9.
[27] B.L. Batista, J.L. Rodrigues, J.A. Nunes, V.C. de Oliveira Souza, F. Barbosa, Exploiting dynamic reaction cell inductively coupled plasma mass spectrometry (DRC-ICP-MS) for sequential determination of trace elements in blood using a dilute-and-shoot procedure, Anal. Chim. Acta 639 (2009) 13–18, https://doi.org/10.1016/j.aca.2009.03.016.